HHS Public Access

Author manuscript

Transl Res. Author manuscript; available in PMC 2023 January 01.

Published in final edited form as:

Transl Res. 2022 January ; 239: 44–57. doi:10.1016/j.trsl.2021.06.002.

Involvement of eNAMPT/TLR4 signaling in murine radiation pneumonitis: protection by eNAMPT neutralization

Alexander N. Garcia[2,^], **Nancy G. Casanova**[1,^], **Daniel G. Valera**[1,^], **Xiaoguang Sun**[1], **Jin H. Song**[1], **Carrie L. Kempf**[1], **Liliana Moreno-Vinasco**[1], **Kimberlie Burns**[1], **Tadeo Bermudez**[1], **Mia Valdez**[1], **Genesis Cuellar**[1], **Taylor Gregory**[1], **Radu C. Oita**[1], **Vivian Reyes Hernon**[1], **Christy Barber**[3], **Sara M. Camp**[1], **Diego Martin**[5], **Zhonglin Liu**[3], **Christian Bime**[1], **Saad Sammani**[1], **Anne E. Cress**[4], **Joe GN Garcia**[1,*]

[1]Department of Medicine, University of Arizona Health Sciences, Tucson, AZ

[2]Department of Radiation Oncology, University of Arizona Health Sciences, Tucson, AZ

[3]Department of Medical Imaging, University of Arizona Health Sciences, Tucson, AZ

[4]Department of Cell and Molecular Medicine, University of Arizona Health Sciences, Tucson, AZ

[5]Department of Radiology and the Translational Imaging Center, Houston Methodist Research Institute, Houston, TX.

Abstract

Therapeutic strategies to prevent or reduce the severity of radiation pneumonitis are a serious unmet need. We evaluated extracellular nicotinamide phosphoribosyltransferase (eNAMPT), a damage-associated molecular pattern protein (DAMP) and Toll-Like Receptor 4 (TLR4) ligand, as a therapeutic target in murine radiation pneumonitis. Radiation-induced murine and human NAMPT expression was assessed *in vitro*, in tissues (IHC, biochemistry, imaging), and in plasma. Wild type C57Bl6 mice (WT) and *Nampt*$^{+/-}$ heterozygous mice were exposed to 20Gy whole thoracic lung irradiation (WTLI) with or without weekly IP injection of IgG_1 (control) or an eNAMPT-neutralizing polyclonal (pAb) or monoclonal antibody (mAb). BAL protein/cells and H&E staining were used to generate a WTLI severity score. Differentially-expressed genes (DEGs)/pathways were identified by RNA sequencing and bioinformatic analyses. Radiation exposure

*Corresponding Author: Joe G. N. Garcia, MD, University of Arizona Health Sciences, Office Phone: (520) 626-1197, skipgarcia@email.arizona.edu.

^Co-first authors

Author Contributions:

JGNG, AEC – conception and design of the work, the analysis and interpretation of data for the work, the drafting and revision of the manuscript, approval of final version to be published ANG, CB, ZL, DM – conception and design of the work, the analysis and interpretation of data for the work, critical revision of key intellectual content and approval of final version to be published.

ANG, DVG, NGC, SMC – collection and analysis of data, revision of the manuscript, and approval of the final version to be published

ANG, JHS, CLK, LMV, KB, TB, MV, GC, SS, RO, VRH, CB – collected data and assisted with processing and manuscript revision

Conflict of Interest Disclosure: Joe GN Garcia MD is CEO and founder of Aqualung Therapeutics Corporation. Aqualung is the manufacturer of the eNAMPT-neutralizing humanized mAb used extensively and suggested as a translational therapy in this report. All other authors declare no competing financial interests. All authors have read the journal's authorship agreement and are in agreement.

increases *in vitro* NAMPT expression in lung epithelium (*NAMPT* promoter activity) and NAMPT lung tissue expression in WTLI-exposed mice. *Nampt*$^{+/-}$ mice and eNAMPT pAb/mAb-treated mice exhibited significant histologic attenuation of WTLI-mediated lung injury with reduced levels of BAL protein and cells, and plasma levels of eNAMPT, IL-6, and IL-1 β. Genomic and biochemical studies from WTLI-exposed lung tissues highlighted dysregulation of NFkB/cytokine and MAP kinase signaling pathways which were rectified by eNAMPT mAb treatment. The eNAMPT/TLR4 pathway is essentially involved in radiation pathobiology with eNAMPT neutralization an effective therapeutic strategy to reduce the severity of radiation pneumonitis.

Abstract

BACKGROUND: Therapeutic strategies to prevent or reduce the severity of exposure to ionizing radiation, occurring either through routine clinical radiotherapy or via nuclear accidents, are a serious medical and societal unmet need. We evaluated extracellular nicotinamide phosphoribosyltransferase (eNAMPT), a damage-associated molecular pattern protein (DAMP) and Toll-Like Receptor 4 (TLR4) ligand, as a therapeutic target in murine radiation pneumonitis.

TRANSLATIONAL SIGNIFICANCE: Preclinical whole thoracic lung irradiation studies support the essential involvement of the eNAMPT/TLR4 signaling pathway in radiation pathobiology. Targeting eNAMPT neutralization with a humanized mAb proved an effective therapeutic strategy to reduce the severity of radiation pneumonitis and potential clinical treatment.

Keywords

whole lung thoracic irradiation; nicotinamide phosphoribosyltransferase; eNAMPT; TLR4; DAMP; RILSS

INTRODUCTION

The development of radiation-induced lung injury (RILI) is a disabling, potentially fatal toxicity in patients undergoing radiotherapy for lung, breast or esophageal cancers or individuals accidentally exposed to ionizing radiation (IR) [1-5]. Radiation pneumonitis is the major dose-limiting toxicity of therapeutic radiotherapy typically developing within 6 weeks post IR exposure. Multiple patient- and treatment-related factors contribute to the risk of radiation pneumonitis including the overall radiation dose, dose-rate fraction size, volume of lung irradiated, co-morbid factors (e.g. emphysema) and genetic factors [6, 7]. Although estimates vary, radiation pneumonitis occurs in >15% of lung cancer patients undergoing radiotherapy [8], adversely limiting radiation dose and/or size of the irradiated volume thereby hindering tumor control.

The pathobiology of radiation pneumonitis is complex but includes IR-stimulated inflammatory responses and reactive oxygen species (ROS) generation resulting in leukocyte infiltration, increased permeability of lung endothelial and epithelial barriers, and impaired gas transfer [5, 9-11]. Radiation-mediated activation of evolutionary-conserved inflammatory pathways, including pathogen-recognition receptors such as the Toll-like receptor family, increases circulating levels of multiple inflammatory cytokines, and

has been implicated in both the development and severity of radiation injury [9, 12]. Unfortunately, experimental and clinical strategies designed to neutralize proinflammatory cytokines and ameliorate IR-induced lung injury have been disappointing [2, 13]. Clinically-useful biomarkers predicting radiation toxicity or responses to potential therapies do not exist [2]. Therapies such as angiotensin-converting-enzyme inhibitors, pentoxyphylline, genistein and antioxidants showed promise in preclinical murine models but failed to show clinical benefit in humans [2, 4, 13] and the cornerstone of clinical care for radiation pneumonitis remains high-dose corticosteroids. Despite acute efficacy, steroids are associated with long term complications and the potential for fatal relapses [2, 3]. Thus, there is a unmet need for effective anti-inflammatory strategies to reduce RILI occurrence and severity.

We previously utilized preclinical murine whole thorax lung irradiation (WTLI) models to explore the role of inflammation in radiation pneumonitis severity and to evaluate potential biomarkers [14], druggable pathways [15] and therapeutic strategies [11, 16-18]. Inhibitors of lung vascular barrier-disrupting kinases such as the non-muscle myosin light chain kinase (nmMLCK) [11] and sphingosine kinase [16], as well as anti-inflammatory agents such as simvastatin [17], and vascular barrier-enhancing agonists such as sphingosine-1-phosphate analogues [18], each reduced the severity of murine radiation pneumonitis. More recently, our preclinical studies of inflammatory lung injury have focused on the role of a cytozyme, nicotinamide phosphoribosyltransferase (NAMPT), as a novel therapeutic inflammatory target in RILI [19-21]. *NAMPT* encodes a cytozyme i.e. an intracellular enzyme (iNAMPT) catalyzing nicotinamide adenine dinucleotide (NAD) synthesis [22] as well as an extracellular cytokine (eNAMPT) [20, 21, 23] that is a damage-associated molecular pattern protein or DAMP via high affinity binding of the pathogen-recognition receptor, Toll-like receptor 4 (TLR4) [12, 24].

We and others have shown that intracellular iNAMPT is a druggable therapeutic target in pulmonary hypertension [25], ARDS [26], and cancer [27, 28], however, enzymatic inhibitors failed in Phase II/Phase III cancer trials due to limited benefit and unacceptable toxicity [29, 30]. In contrast, our studies have focused on the novel DAMP functions of secreted eNAMPT to profoundly amplify potent evolutionarily-conserved inflammatory networks that produce increased cytokine burden, organ dysfunction, and potentially death [12]. eNAMPT is a novel therapeutic target and plasma biomarker in ARDS/ventilator-induced lung injury (VILI) [12, 19-21, 31-33], in pulmonary arterial hypertension [25, 34], in prostate cancer [35] and in inflammatory bowel disease [36].

Our current studies, designed to explore the role of eNAMPT in radiation pneumonitis, revealed markedly increased eNAMPT expression and secretion in IR-exposed humans and mice. Utilizing a humanized eNAMPT-neutralizing mAb to potentially address an unmet medical need, we demonstrate that eNAMPT/TLR4 signaling is a highly druggable therapeutic target and essential contributor to WTLI-induced radiation pneumonitis.

MATERIALS AND METHODS

Reagents.

All reagents were purchased from Sigma-Aldrich (St. Louis, MO) unless otherwise noted in Supplemental Materials and Methods. Akt tyrosine nitration (Y^{350} NO_2) antibody [19] and the anti-human eNAMPT polyclonal pAb were generated as previously reported [20]. Details of the eNAMPT-neutralizing humanized mAb (ALT-100, Aqualung Therapeutics, Tucson, AZ) have been previously reported [21].

NAMPT Promoter Luciferase Reporter Activity Assay.

Previously described plasmid constructs containing a 3 kb segment of the *NAMPT* gene promoter (−3,028 bp to +1 ATG) and the Renilla luciferase reporter [23, 34] were transfected into human pulmonary endothelial cells (HPAEC), human bronchial epithelial cell lines (HBE, BEAS), and human lung fibroblast cells (IMR-90). Transfected cells were exposed to 8 Gy ionizing radiation for 1, 4, 24 and 48 hours and luciferase activity measured and normalized by Renilla luciferase activity [23, 34].

Murine Studies.

The work contained in this manuscript conforms to the ethical guidelines for human and animal research. Mice were housed under standard conditions with all procedures and experiments approved by the Institutional Animal Care and Use Committee (University of Arizona). Experiments utilized either wild type male C57BL/6J mice (20-25 g) (8–12 weeks, Jackson Laboratories, Bar Harbor, ME), or *Nampt*$^{+/-}$ heterozygous mice generated as we previously described [20, 25] (see Supplemental Materials and Methods).

Whole Thoracic Lung Radiation (WTLI)-Induced Lung Injury:

Wild type (WT) and *Nampt*$^{+/-}$ heterozygous mice or litter-mate controls, were anesthetized with ketamine (65 mg/kg), xylazine (10mg/kg) and acepromazine (2 mg/kg) and exposed to WTLI radiation (20 Gy) as described previously [17, 18] (Supplemental Materials and Methods).

Imaging of NAMPT Tissue Expression.

An eNAMPT-binding humanized mAb (Aqualung Therapeutics, Tucson, AZ) was radiolabeled with ^{99m}Tc to produce a specific probe (^{99m}Tc-ProNamptor™) for *in vivo* imaging of NAMPT expression in WTLI-exposed pulmonary tissues. To verify ^{99m}Tc-ProNamptor™ specificity, human IgG was labeled with ^{99m}Tc (^{99m}Tc-IgG). ^{99m}Tc-ProNamptor™ or ^{99m}Tc-IgG (1.0 mCi) was intravenously injected into C57BL/6J mice 1 week after WTLI exposure. A separate group of mice receiving no radiation treatment, served as additional controls. All mice were anesthetized with 1% isoflurane and imaged at 30-240 minutes after radiotracer injection using a Quantum Imaging Detector (iQID) camera [37-43]. At the conclusion of each whole-body imaging session, mice were euthanized and lungs harvested for radioactivity-based measurements of ^{99m}Tc-ProNamptor™ biodistribution and *ex vivo* autoradiography as we described previously [21].

Bronchoalveolar lavage (BAL) Analysis.

Bronchoalveolar lavage was performed as we have previously described [21] with BAL fluid retrieval, protein analysis, and cell count analysis including PMN determinations (Supplemental Materials and Methods).

Quantitative Lung Histology and Immunohistochemistry Staining.

Lungs were fixed in 10% formalin and processed for H&E or immunohistochemistry staining for NAMPT with primary or IgG isotype control, as previously described [21]. Histological and IHC images were randomly selected for H&E and NAMPT quantification using ImageJ software as described previously [21] (Supplemental Materials and Methods).

Radiation-Induced Lung Injury Severity Score (RILSS) Quantification.

A ranking point system, the Radiation-Induced Lung Injury Severity Score (RILSS) incorporating published recommendations [44], was utilized to integrate WTLI injury indices in preclinical models and facilitate statistical comparisons. A score is objectively assigned to each animal for each of 3 readouts of inflammation (BAL protein, BAL total cell count, H&E histology quantification) on a scale from 1 to 5 points for a maximal score of 15 points. RILSS scores of 4 or less reflect the absence of injury, scores of 5-8 points reflect mild injury, scores of 9-12 points reflect moderate injury, and scores 13-15 points reflect severe injury (Supplemental Materials and Methods).

Biochemical Analyses of Human and Murine Cells/Tissues.

Lung tissue homogenates/cell lysates were utilized for Western blotting as previously described [21] with densitometric quantification of lung tissue expressed proteins, including NAMPT, with β-actin normalization (Supplemental Materials and Methods).

Plasma Cytokine Measurements.

Human plasma eNAMPT levels were measured with an in house ELISA as we previously reported [32, 34, 45]. Plasma levels of eNAMPT, IL-6, and IL-1β from 20 Gy-exposed mice were measured utilizing a meso-scale ELISA platform (Meso Scale Diagnostics, Rockville, MD) as previously described [21] (Supplemental Materials and Methods).

Lung Tissue RNAseq Analysis.

Total RNA was extracted from control and WTLI-exposed lung tissues with RNA QC as previously described [18]. Mouse RNA was sequenced using the using BGISEQ platform. Bowtie2 [46] was utilized to map clean reads, and expression levels calculated with RSEM [47]. Pearson correlations were calculated to reflect correlation between samples. DEseq2 [48] algorithms were used to detect the differentially-expressed genes (DEGs). To control for multiple testing error, a False Discovery Rate (FDR) of 0.05 was applied to identify significantly-enriched pathways for each gene module identified by the unsupervised analysis. Enrichment analysis for Gene Ontology (GO) classification focused on biological process and pathway classification. Statistically-significant DEGs for each comparison underwent unbiased comparison of the DE gene sets to ConsensusPathDB [47] using the over-representation gene set analysis against the pathway databases with

the Kyoto Encyclopedia of Genes and Genomes (KEGG) [49] and Reactome [50]. The STRING [51] database analyzed the protein and protein interactions to construct the interaction networks and Gene Ontology (GO) of the DEGs and pathway analysis with the KEGG and Reactome datasets publicly available on the GEO database (http://www.ncbi.nlm.nih.gov/geo/) (Supplement Material and Methods).

Statistical analysis.

Two-way ANOVA was used to compare the means of data from two or more different experimental groups. If significant difference was present by ANOVA ($p < 0.05$), a least significant differences test was performed post hoc. Subsequently, differences between groups were considered statistically significant when $p < 0.05$.

RESULTS

Ionizing radiation increases NAMPT expression in human cells and murine lung tissues.

Initial studies designed to assess NAMPT involvement in human responses to radiation revealed marked NAMPT expression in normal human cells transfected with a *NAMPT* luciferase reporter promoter and exposed to one dose of 8 Gy. The *NAMPT* promoter luciferase assay does not distinguish between iNAMPT and eNAMPT but temporally reflects initial iNAMPT generation with eNAMPT secretion a subsequent event. Compared to controls, 8 Gy exposure significantly increased *NAMPT* promoter activity in human lung endothelium, lung epithelium, and fibroblasts, beginning at 4 hours post exposure and persiting at 48 hours (Figure 1A/B). Significant time-dependent increases in NAMPT protein expression in 8 Gy-exposed human lung endothelium was observed at 24 and 48 hrss post exposure (Figure 1C). In an established 20 Gy WTLI murine model of radiation pneumonitis[11, 14-18] we observed demonstrated significant time-dependent increases in NAMPT expression at 1 and 4 weeks (Figure 1D/E). These immunohistochemistry studies were validated by biochemical studies of NAMPT protein immuno-reactivity in WTLI-exposed lung homogenates (1, 2 and 4 weeks, Figure1F).

In vivo NAMPT imaging detects NAMPT expression in murine radiation pneumonitis.

WTLI-induced increases in lung tissue NAMPT expression were further confirmed non-invasively utilizing a radiolabeled anti-eNAMPT mAb probe (^{99m}Tc-ProNamptor™) as previously reported [21]. Whole-body ^{99m}Tc-ProNamptor™ imaging of WTLI-exposed mice at 1 week showed significant time-dependent increases in lung probe uptake compared to ^{99m}Tc-IgG controls. Within the chest region of interest in WTLI-exposure mice, ^{99m}Tc-ProNamptor™ radioactivity was initially predominately localized to the cardiac blood pool (30 minutes post probe injection) but significantly accumulated in lung tissues by 2 hours and remained persistently greater than ^{99m}Tc-IgG control mice after 4 hours (Figure 2A). *In vivo* quantitative image analysis, auto-radiography, and *ex vivo* lung radioactive measurements validated the accuracy of *in vivo* quantitative lung activity measurements (Figures 2B-D). It is important to note that that the eNAMPT imaging probe may reflect a combination of iNAMPT and eNAMPT detected expression.

eNAMPT neutralization reduces the severity of preclinical radiation pneumonitis.

Similar to prior p studies of WTLI pneumonitis [14-18], 20 Gy WTLI-exposed mice exhibited marked lung inflammatory injury beginning at 1 week, significantly increasing at 4 weeks, characterized histologically by dramatic increases in inflammation cell infiltration, vascular leakage with alveolar edema and injury (Figure 3A) quantified by Image J software analysis (Figure 3B). WTLI produced significant increases in BAL indices of inflammation (total BAL protein and cells) (Figures 3C/D) which were combined into the Radiation-Induced Lung Injury Severity Score (RILISS) showing significant lung injury at both 1 and 4 weeks post WTLI (Figure 3E).

To explore eNAMPT as a direct participant in the pathobiology of WTLI radiation pneumonitis, we next neutralized circulating eNAMPT with either a polyclonal (pAb) or humanized monoclonal antibody (mAb), a strategy which ameliorates inflammatory injury in preclinical models of ARDS [19-21], pulmonary hypertension [34] and prostate cancer [35]. Intraperitoneal delivery of either the eNAMPT pAb or mAb, beginning day 1 after WTLI and continued weekly thereafter, significantly reduced WTLI-mediated histologic injury and increases in BAL protein and cells (Figure 3), an overall 60% RILISS reduction (Figure 3E) with protection greater with the humanized eNAMPT mAb compared to the eNAMPT pAb. The eNAMPT-neutralizing mAb also significantly reduced WTLI-induced increases in plasma levels of eNAMPT, IL-6 and IL-1 β at 4 weeks (Figure 3F/G/H).

Preclinical murine radiation pneumonitis is reduced in *Nampt*$^{+/-}$ heterozygous mice.

As mice with homozygous *NAMPT* deletion experience embryonic lethality, we previously utilized *Nampt*$^{+/-}$ heterozygous mice to validate NAMPT as a therapeutic target in preclinical models of ARDS [20, 24] and PAH [25]. Assessment of WTLI-exposed *Nampt*$^{+/-}$ mice at 4 weeks revealed significant attenuation of histological lung injury (Figure 4A/B), BAL inflammatory indices (Figure 4C/D), and the RILISS severity score (Figure 4E), confirming eNAMPT involvement in the development and severity of radiation pneumonitis.

Differentially-expressed gene/pathway expression in preclinical murine radiation pneumonitis: rectification by an eNAMPT mAb.

We further assessed the role of circulating eNAMPT in driving WTLI-induced lung injury by examining the WTLI -mediated dysregulation of lung inflammatory signaling and injury/repair processes, initially by comparing RNA sequencing data from sham- and WTLI-exposed mice. A total of 2325 differentially-expressed genes (DEGs) genes with a FDR of <0.05 were filtered to 337 DEGs which exhibited a fold change (FC) of >1.5 or <1.5 with top DEGs depicted in a volcano plot (Figure 5A). Integrating these DEG data into GO biologic processes pathways identified significant WTLI-mediated dysregulation of genes/pathways involved in leukocyte migration, chemokine signaling, ion homeostasis, and both cytokine- and MAP kinase-induced signaling (Figure 5B). Inserting these DEGs into the KEGG/Reactome database revealed oxidative phosphorylation, cancer-related pathways, p53-, Rho GTPase- and chemokine-signaling as the most significant pathways (Table 1).

We next assessed the most significantly dysregulated DEGs in lung tissues from WTLI-exposed mice (4 weeks) receiving either IgG_1 or the eNAMPT mAb which identified far fewer DEGs (207 DEGs) than the comparison of sham vs WTLI-elicited DEGs, as well as reduced level of expression of the top DEGs (Figure 5C). The STRING-based interactome of top prioritized DEGs, shown in Figure 5D, highlights IL-1 β as a central hub gene, consistent with the effect of the eNAMPT-neutralizing mAb on plasma levels of IL-1 β (Figure 3H). Integrating DEG data into top STRING GO-related terms (Table 2) and KEGG/Reactome pathways (Table 3) identified mAb-influenced pathways related to Toll-like receptor 4 binding, MHC class II protein binding, Innate immunity, Neutrophil degranulation, Leukocyte transmigration, and ROS detoxification.

eNAMPT neutralization rectifies dysregulated NFkB and MAP kinase signaling pathways in preclinical radiation pneumonitis.

Biochemical studies were conducted to confirm eNAMPT's influence on WTLI-induced dysregulated signaling identified by differentially-expressed transcriptomic changes. Marked increases in the activation/ phosphorylation of NFkB (Figure 6A) and MAP kinase family members (ERK, p-38, JNK) (Figure 6B) were observed in lung homogenates from WTLI-challenged mice. The strong WTLI-induced dysregulation of NFkB and MAP kinase family signaling pathways were marked rectified in WTLI-challenged mice receiving the eNAMPT-neutralizing mAb. These studies are consistent with a potentially important role for the eNAMPT/TLR4 pathway in triggering WTLI-induced inflammatory cascades that contribute to the severity of WTLI-mediated lung injury.

DISCUSSION

Radiation pneumonitis is a debilitating and potentially fatal complication of radiotherapy, occurring in >15% of cancer patients, or in accidental exposures to ionizing radiation. Beyond the inherent morbidity and mortality of radiation pneumonitis in patients undergoing radiotherapy [8], the development of radiation pneumonitis also compromises and delays curative or remission-inducing treatments [1-5]. The possibility of nuclear accidents or potential acts of terrorism, have also heightened concern for catastrophic radiation-induced multiorgan failure, including pneumonitis. A single 8Gy exposure was lethal in 50% of radiation accident-exposed victims with pneumonitis developing in ~30% of exposed patients (including fatal pneumonitis) [52, 53]. Effective therapeutic mitigators for radiation exposure do not currently exist, highlighting a serious unmet medical and societal need. Multiple studies of prophylactic steroid administration, the cornerstone of standard therapy for radiation pneumonitis, found little benefit while potentially prolonging the duration of pneumonitis [2, 54].

Despite the complexity of radiation pneumonitis pathobiology (DNA damage, oxidative stress, cellular senescence), inflammation is a primary contributor to the severity of this radiation toxicity [5, 9]. The current study strongly indicates that eNAMPT serves as both an indicator of radiation injury and is essentially involved in the severity of WTLI-induced pneumonitis. Our preliminary studies in human cancer subjects undergoing radiotherapy for

lung cancer indicate eNAMPT levels are increased ~4 fold in cancer subjects with radiation pneumonitis compared to healthy controls (data not shown).

We have previously shown circulating eNAMPT is a DAMP which activates evolutionarily-conserved, NFκB-inducible inflammatory cascades via ligation of the pathogen-recognition receptor, TLR4 [24]. Our prior studies indicate that eNAMPT/TLR4 signaling contributes to multiorgan failure and ARDS pathobiology/mortality [12, 19-21] and to the pathobiologies of pulmonary hypertension [25, 34, 55] and prostate cancer [35]. Our current studies unequivocally demonstrate radiation exposure as a potent stimulus for NAMPT expression in both human and murine tissues, findings corroborated by preclinical biochemical studies, IHC studies and *in vivo* lung imaging utilizing a radiolabeled-eNAMPT mAb probe (^{99m}Tc-ProNamptor™) [21]. eNAMPT involvement in radiation pneumonitis is further supported by the reduced IR-induced injury observed in *Nampt*$^{+/-}$ heterozygous mice and by the striking efficacy of eNAMPT neutralization (pAb/mAb) in attenuating inflammatory parameters and lung injury severity including circulating levels of the cytokines IL-6 and IL-1β. The availability of an eNAMPT-neutralizing humanized mAb as a potential biologic therapy for cancer patients undergoing radiotherapy or individuals exposed to total or partial body irradiation (as in a nuclear incident) may potentially address this serious unmet need.

The exact mechanism of radiation-induced *NAMPT* transcription and protein expression/secretion is unknown, however, our studies have previously shown the involvement of genetic and epigenetic factors, mechanical stress, hypoxia and growth factors [23, 34, 56, 57]. Although not directly explored in the current study, we have previously shown that transcription factors associated with radiation responses (STAT family, SOX family, NRF2, NFkB, HIF2α) [58], each contribute to *NAMPT* transcription and secretion [23, 34, 57]. We previously identified several *NAMPT* promoter SNPs with increased minor allelic frequency in both European and African descent populations (> 0.01) that influence transcription factor binding and DNA methylation [23, 56, 57] and which confer risk and severity of acute inflammatory lung injury [31, 33, 34]. Interestingly, while genetic studies focused on susceptibility variants for radiation pneumonitis are limited, several risk SNPs in specific inflammatory, fibrotic and DNA repair candidate genes have been reported in a Chinese Han population [59-63]. It will be interesting to determine if *NAMPT* promoter SNPs that influence eNAMPT plasma levels [64] also confer susceptibility to the development of radiation pneumonitis and WTLI severity in both ethnic-specific and diverse racial populations.

Complementing our preclinical pathophysiologic studies, we conducted highly targeted genomic and biochemical explorations designed to decipher events involved in the initiation and progression of radiation pneumonitis. These studies confirmed our prior reports [18] that highlighted dysregulated ROS/oxidative phosphorylation, MAP kinase, chemokine/cytokine-mediated signaling pathways and leukocyte migration in the murine radiation pneumonitis model. Of interest, biochemical and genomic results confirmed eNAMPT mAb-mediated rectification of TLR4/NFkB and MAP kinase family dysregulated signaling pathways, validated by biochemical detection of reduced phosphorylation/activation of MAP kinase family and NFkB proteins. The eNAMPT mAb strongly rectified dysregulated IL-1β expression, a potent proinflammatory cytokine and major mediator of neutrophil influx and

activation and T-cell activation/cytokine production. Consistent with eNAMPT mAb effects on IL-1β-related DEG interactions, weekly treatment with the eNAMPT mAb significantly reduced circulating plasma IL-1β levels in WTLI-exposed mice.

In summary, our combined human and murine studies, utilizing a well-established highly informative murine WTLI model [11, 14-18, 65], support secreted eNAMPT, a DAMP and ligand for the pattern-recognition receptor, TLR4 as a highly druggable therapeutic target in radiation pneumonitis. Our data indicate the humanized eNAMPT-neutralizing mAb as a potential therapeutic strategy for significantly reducing the severity of or preventing the development of radiation pneumonitis. We speculate that as a biologic therapy, the eNAMPT mAb will exhibit minimal off target effects and antigenicity, and prove safer and of superior efficacy when compared to standard care with high dose corticosteroids (preclinical studies that are underway). As we identified plasma eNAMPT plasma levels as a potentially valuable biomarker for development of radiation pneumonitis, the potential for combining plasma eNAMPT levels, with specific disease-risk *NAMPT* genotypes [23, 33, 34, 64], may allow for identification of individuals undergoing radiotherapy at high risk for developing radiation pneumonitis and most likely to respond to humanized eNAMPT-neutralizing mAb therapy, a strategy that provides a personalized approach to radiation pneumonitis.

Supplementary Material

Refer to Web version on PubMed Central for supplementary material.

Acknowledgments

All named authors have read the journal's authorship agreement and have reviewed and approved the manuscript.

Funding:

NIH Grants R01 HL094394, P01 HL134610, R42 HL152888.

REFERENCES

[1]. Giuranno L, Ient J, De Ruysscher D, Vooijs MA. Radiation-Induced Lung Injury (RILI). Front Oncol. 2019;9:877. [PubMed: 31555602]

[2]. Hanania AN, Mainwaring W, Ghebre YT, Hanania NA, Ludwig M. Radiation-Induced Lung Injury: Assessment and Management. Chest. 2019;156:150–62. [PubMed: 30998908]

[3]. Keffer S, Guy CL, Weiss E. Fatal Radiation Pneumonitis: Literature Review and Case Series. Adv Radiat Oncol. 2020;5:238–49. [PubMed: 32280824]

[4]. Mehta V Radiation pneumonitis and pulmonary fibrosis in non-small-cell lung cancer: pulmonary function, prediction, and prevention. Int J Radiat Oncol Biol Phys. 2005;63:5–24. [PubMed: 15963660]

[5]. Yarnold J, Brotons MC. Pathogenetic mechanisms in radiation fibrosis. Radiother Oncol. 2010;97:149–61. [PubMed: 20888056]

[6]. Morgan GW, Breit SN. Radiation and the lung: a reevaluation of the mechanisms mediating pulmonary injury. Int J Radiat Oncol Biol Phys. 1995;31:361–9. [PubMed: 7836090]

[7]. Roberts CM, Foulcher E, Zaunders JJ, Bryant DH, Freund J, Cairns D, et al. Radiation pneumonitis: a possible lymphocyte-mediated hypersensitivity reaction. Ann Intern Med. 1993;118:696–700. [PubMed: 8460855]

[8]. Rodrigues G, Lock M, D'Souza D, Yu E, Van Dyk J. Prediction of radiation pneumonitis by dose - volume histogram parameters in lung cancer--a systematic review. Radiother Oncol. 2004;71:127–38. [PubMed: 15110445]

[9]. Lierova A, Jelicova M, Nemcova M, Proksova M, Pejchal J, Zarybnicka L, et al. Cytokines and radiation-induced pulmonary injuries. J Radiat Res. 2018;59:709–53. [PubMed: 30169853]

[10]. Osterreicher J, Pejchal J, Skopek J, Mokry J, Vilasova Z, Psutka J, et al. Role of type II pneumocytes in pathogenesis of radiation pneumonitis: dose response of radiation-induced lung changes in the transient high vascular permeability period. Exp Toxicol Pathol. 2004;56:181–7. [PubMed: 15625787]

[11]. Wang T, Mathew B, Wu X, Shimizu Y, Rizzo AN, Dudek SM, et al. Nonmuscle myosin light chain kinase activity modulates radiation-induced lung injury. Pulm Circ. 2016;6:234–9. [PubMed: 27252850]

[12]. Bime C, Casanova NG, Nikolich-Zugich J, Knox KS, Camp SM, Garcia JGN. Strategies to DAMPen COVID-19-mediated lung and systemic inflammation and vascular injury. Transl Res. 2020:S1931.

[13]. Sio TT, Atherton PJ, Pederson LD, Zhen WK, Mutter RW, Garces YI, et al. Daily Lisinopril vs Placebo for Prevention of Chemoradiation-Induced Pulmonary Distress in Patients With Lung Cancer (Alliance MC1221): A Pilot Double-Blind Randomized Trial. Int J Radiat Oncol Biol Phys. 2019;103:686–96. [PubMed: 30395904]

[14]. Mathew B, Jacobson JR, Siegler JH, Moitra J, Blasco M, Xie L, et al. Role of migratory inhibition factor in age-related susceptibility to radiation lung injury via NF-E2-related factor-2 and antioxidant regulation. American journal of respiratory cell and molecular biology. 2013;49:269–78. [PubMed: 23526214]

[15]. Mathew B, Takekoshi D, Sammani S, Epshtein Y, Sharma R, Smith BD, et al. Role of GADD45a in murine models of radiation- and bleomycin-induced lung injury. American journal of physiology Lung cellular and molecular physiology. 2015;309:L1420–9. [PubMed: 26498248]

[16]. Gorshkova I, Zhou T, Mathew B, Jacobson JR, Takekoshi D, Bhattacharya P, et al. Inhibition of serine palmitoyltransferase delays the onset of radiation-induced pulmonary fibrosis through the negative regulation of sphingosine kinase-1 expression. Journal of lipid research. 2012;53:1553–68. [PubMed: 22615416]

[17]. Mathew B, Huang Y, Jacobson JR, Berdyshev E, Gerhold LM, Wang T, et al. Simvastatin attenuates radiation-induced murine lung injury and dysregulated lung gene expression. American journal of respiratory cell and molecular biology. 2011;44:415–22. [PubMed: 20508068]

[18]. Mathew B, Jacobson JR, Berdyshev E, Huang Y, Sun X, Zhao Y, et al. Role of sphingolipids in murine radiation-induced lung injury: protection by sphingosine 1-phosphate analogs. FASEB journal : official publication of the Federation of American Societies for Experimental Biology. 2011;25:3388–400. [PubMed: 21712494]

[19]. Bermudez T, Sammani S, Song JH, Valera DG, Reyes Hernon V, Valera DG, et al. eNAMPT neutralization reduces preclinical ARDS severity via rectified NFkB and Akt/mTORC2 signaling. Sci Rep. 2021 (submitted).

[20]. Hong SB, Huang Y, Moreno-Vinasco L, Sammani S, Moitra J, Barnard JW, et al. Essential role of pre-B-cell colony enhancing factor in ventilator-induced lung injury. American journal of respiratory and critical care medicine. 2008;178:605–17. [PubMed: 18658108]

[21]. Quijada H, Bermudez T, Kempf CL, Valera DG, Garcia AN, Camp SM, et al. Endothelial eNAMPT Amplifies Preclinical Acute Lung Injury: Efficacy of an eNAMPT-Neutralising mAb. Eur Respir J. 2020:2002536.

[22]. Wang T, Zhang X, Bheda P, Revollo JR, Imai S-i, Wolberger C. Structure of Nampt/PBEF/visfatin, a mammalian NAD+ biosynthetic enzyme. Nature Structural & Molecular Biology. 2006;13:661.

[23]. Sun X, Elangovan VR, Mapes B, Camp SM, Sammani S, Saadat L, et al. The NAMPT promoter is regulated by mechanical stress, signal transducer and activator of transcription 5, and acute respiratory distress syndrome-associated genetic variants. American journal of respiratory cell and molecular biology. 2014;51:660–7. [PubMed: 24821571]

[24]. Camp SM, Ceco E, Evenoski CL, Danilov SM, Zhou T, Chiang ET, et al. Unique Toll-Like Receptor 4 Activation by NAMPT/PBEF Induces NFkappaB Signaling and Inflammatory Lung Injury. Sci Rep. 2015;5:13135. [PubMed: 26272519]

[25]. Chen J, Sysol JR, Singla S, Zhao S, Yamamura A, Valdez-Jasso D, et al. Nicotinamide Phosphoribosyltransferase Promotes Pulmonary Vascular Remodeling and Is a Therapeutic Target in Pulmonary Arterial Hypertension. Circulation. 2017;135:1532–46. [PubMed: 28202489]

[26]. Moreno-Vinasco L, Quijada H, Sammani S, Siegler J, Letsiou E, Deaton R, et al. Nicotinamide phosphoribosyltransferase inhibitor is a novel therapeutic candidate in murine models of inflammatory lung injury. American journal of respiratory cell and molecular biology. 2014;51:223–8. [PubMed: 24588101]

[27]. Audrito V, Manago A, Gaudino F, Sorci L, Messana VG, Raffaelli N, et al. NAD-Biosynthetic and Consuming Enzymes as Central Players of Metabolic Regulation of Innate and Adaptive Immune Responses in Cancer. Front Immunol. 2019;10:1720. [PubMed: 31402913]

[28]. Galli U, Colombo G, Travelli C, Tron GC, Genazzani AA, Grolla AA. Recent Advances in NAMPT Inhibitors: A Novel Immunotherapic Strategy. Front Pharmacol. 2020;11:656. [PubMed: 32477131]

[29]. Roulston A, Shore GC. New strategies to maximize therapeutic opportunities for NAMPT inhibitors in oncology. Mol Cell Oncol. 2016;3:e1052180. [PubMed: 27308565]

[30]. von Heideman A, Berglund A, Larsson R, Nygren P. Safety and efficacy of NAD depleting cancer drugs: results of a phase I clinical trial of CHS 828 and overview of published data. Cancer Chemother Pharmacol. 2010;65:1165–72. [PubMed: 19789873]

[31]. Bajwa EK, Yu CL, Gong MN, Thompson BT, Christiani DC. Pre-B-cell colony-enhancing factor gene polymorphisms and risk of acute respiratory distress syndrome. Crit Care Med. 2007;35:1290–5. [PubMed: 17414088]

[32]. Bime C, Casanova N, Oita RC, Ndukum J, Lynn H, Camp SM, et al. Development of a biomarker mortality risk model in acute respiratory distress syndrome. Crit Care. 2019;23:410. [PubMed: 31842964]

[33]. Ye SQ, Simon BA, Maloney JP, Zambelli-Weiner A, Gao L, Grant A, et al. Pre-B-cell colony-enhancing factor as a potential novel biomarker in acute lung injury. American journal of respiratory and critical care medicine. 2005;171:361–70. [PubMed: 15579727]

[34]. Sun X, Sun BL, Babicheva A, Vanderpool R, Oita RC, Casanova N, et al. Direct Extracellular NAMPT Involvement in Pulmonary Hypertension and Vascular Remodeling. Transcriptional Regulation by SOX and HIF-2alpha. American journal of respiratory cell and molecular biology. 2020;63:92–103. [PubMed: 32142369]

[35]. Sun BL, Sun X, Casanova N, Garcia AN, Oita R, Algotar AM, et al. Role of secreted extracellular nicotinamide phosphoribosyltransferase (eNAMPT) in prostate cancer progression: Novel biomarker and therapeutic target. EBioMedicine. 2020;61:103059. [PubMed: 33045468]

[36]. Colombo G, Clemente N, Zito A, Bracci C, Colombo FS, Sangaletti S, et al. Neutralization of extracellular NAMPT (nicotinamide phosphoribosyltransferase) ameliorates experimental murine colitis. J Mol Med (Berl). 2020;98:595–612. [PubMed: 32338310]

[37]. Lamart S, Miller BW, Van der Meeren A, Tazrart A, Angulo JF, Griffiths NM. Actinide bioimaging in tissues: Comparison of emulsion and solid track autoradiography techniques with the iQID camera. PLoS One. 2017;12:e0186370. [PubMed: 29023595]

[38]. Frost SH, Miller BW, Back TA, Santos EB, Hamlin DK, Knoblaugh SE, et al. alpha-Imaging Confirmed Efficient Targeting of CD45-Positive Cells After 211At-Radioimmunotherapy for Hematopoietic Cell Transplantation. J Nucl Med. 2015;56:1766–73. [PubMed: 26338894]

[39]. Barber HB, Fastje D, Lemieux D, Grim GP, Furenlid LR, Miller BW, et al. Imaging properties of pixellated scintillators with deep pixels. Proc SPIE Int Soc Opt Eng. 2014;9215.

[40]. Miller BW, Gregory SJ, Fuller ES, Barrett HH, Barber HB, Furenlid LR. The iQID camera: An ionizing-radiation quantum imaging detector. Nucl Instrum Methods Phys Res A. 2014;767:146–52. [PubMed: 26166921]

[41]. Furenlid LR, Barrett HH, Barber HB, Clarkson EW, Kupinski MA, Liu Z, et al. Molecular Imaging in the College of Optical Sciences - An Overview of Two Decades of Instrumentation Development. Proc SPIE Int Soc Opt Eng. 2014;9186.

[42]. Han L, Miller BW, Barber HB, Nagarkar VV, Furenlid LR. A New Columnar CsI(Tl) Scintillator for iQID detectors. Proc SPIE Int Soc Opt Eng. 2014;9214:92140D.

[43]. Miller BW, Frost SH, Frayo SL, Kenoyer AL, Santos E, Jones JC, et al. Quantitative single-particle digital autoradiography with alpha-particle emitters for targeted radionuclide therapy using the iQID camera. Med Phys. 2015;42:4094–105. [PubMed: 26133610]

[44]. Matute-Bello G, Downey G, Moore BB, Groshong SD, Matthay MA, Slutsky AS, et al. An official American Thoracic Society workshop report: features and measurements of experimental acute lung injury in animals. American journal of respiratory cell and molecular biology. 2011;44:725–38. [PubMed: 21531958]

[45]. Oita RC, Camp SM, Ma W, Ceco E, Harbeck M, Singleton P, et al. Novel Mechanism for Nicotinamide Phosphoribosyltransferase Inhibition of TNF-alpha-mediated Apoptosis in Human Lung Endothelial Cells. American journal of respiratory cell and molecular biology. 2018;59:36–44. [PubMed: 29337590]

[46]. Langmead B, Salzberg SL. Fast gapped-read alignment with Bowtie 2. Nat Methods. 2012;9:357–9. [PubMed: 22388286]

[47]. Kamburov A, Stelzl U, Lehrach H, Herwig R. The ConsensusPathDB interaction database: 2013 update. Nucleic Acids Res. 2013;41:D793–800. [PubMed: 23143270]

[48]. Cock PJ, Fields CJ, Goto N, Heuer ML, Rice PM. The Sanger FASTQ file format for sequences with quality scores, and the Solexa/Illumina FASTQ variants. Nucleic Acids Res. 2010;38:1767–71. [PubMed: 20015970]

[49]. Du J, Yuan Z, Ma Z, Song J, Xie X, Chen Y. KEGG-PATH: Kyoto encyclopedia of genes and genomes-based pathway analysis using a path analysis model. Mol Biosyst. 2014;10:2441–7. [PubMed: 24994036]

[50]. Fabregat A, Sidiropoulos K, Viteri G, Forner O, Marin-Garcia P, Arnau V, et al. Reactome pathway analysis: a high-performance in-memory approach. BMC Bioinformatics. 2017;18:142. [PubMed: 28249561]

[51]. Szklarczyk D, Morris JH, Cook H, Kuhn M, Wyder S, Simonovic M, et al. The STRING database in 2017: quality-controlled protein-protein association networks, made broadly accessible. Nucleic acids research. 2017;45:D362–D8. [PubMed: 27924014]

[52]. (UNSCEAR). UNSCotEoAR. Report to the General Assembly, Annex J: Exposure and Effects of the Chernobyl Accident. Sources, effects and risks of ionizing radiation. 2000.

[53]. DiCarlo AL, Jackson IL, Shah JR, Czarniecki CW, Maidment BW, Williams JP. Development and licensure of medical countermeasures to treat lung damage resulting from a radiological or nuclear incident. Radiat Res. 2012;177:717–21. [PubMed: 22468704]

[54]. Mahmood J, Jelveh S, Calveley V, Zaidi A, Doctrow SR, Hill RP. Mitigation of lung injury after accidental exposure to radiation. Radiat Res. 2011;176:770–80. [PubMed: 22013884]

[55]. Ahmed M, Zaghloul N, Zimmerman P, Casanova NG, Sun X, Reyes Hernon V, et al. Endothelial eNAMPT drives EndMT and preclinical PH: Rescue by an eNAMPT-neutralizing mAb. Am J Resp Cell Mol Biol. 2021 (submitted).

[56]. Adyshev DM, Elangovan VR, Moldobaeva N, Mapes B, Sun X, Garcia JG. Mechanical stress induces pre-B-cell colony-enhancing factor/NAMPT expression via epigenetic regulation by miR-374a and miR-568 in human lung endothelium. American journal of respiratory cell and molecular biology. 2014;50:409–18. [PubMed: 24053186]

[57]. Elangovan VR, Camp SM, Kelly GT, Desai AA, Adyshev D, Sun X, et al. Endotoxin- and mechanical stress–induced epigenetic changes in the regulation of the nicotinamide phosphoribosyltransferase promoter. Pulmonary Circulation. 2016;6:539–44. [PubMed: 28090296]

[58]. Emmerson E, May AJ, Berthoin L, Cruz-Pacheco N, Nathan S, Mattingly AJ, et al. Salivary glands regenerate after radiation injury through SOX2-mediated secretory cell replacement. EMBO Mol Med. 2018;10. [PubMed: 29191946]

[59]. Liu B, Tang Y, Yi M, Liu Q, Xiong H, Hu G, et al. Genetic variants in the plasminogen activator inhibitor-1 gene are associated with an increased risk of radiation pneumonitis in lung cancer patients. Cancer Med. 2017;6:681–8. [PubMed: 28211612]

[60]. Liu B, Yi M, Tang Y, Liu Q, Qiu H, Zou Y, et al. MMP-1 promoter polymorphism is associated with risk of radiation-induced lung injury in lung cancer patients treated with radiotherapy. Oncotarget. 2016;7:70175–84. [PubMed: 27659527]

[61]. Wen J, Liu H, Wang L, Wang X, Gu N, Liu Z, et al. Potentially Functional Variants of ATG16L2 Predict Radiation Pneumonitis and Outcomes in Patients with Non-Small Cell Lung Cancer after Definitive Radiotherapy. J Thorac Oncol. 2018;13:660–75. [PubMed: 29454863]

[62]. Xiao Y, Yuan X, Qiu H, Li Q. Single-nucleotide polymorphisms of TGFbeta1 and ATM associated with radiation-induced pneumonitis: a prospective cohort study of thoracic cancer patients in China. Int J Clin Exp Med. 2015;8:16403–13. [PubMed: 26629166]

[63]. Yi M, Tang Y, Liu B, Li Q, Zhou X, Yu S, et al. Genetic variants in the ITGB6 gene is associated with the risk of radiation pneumonitis in lung cancer patients treated with thoracic radiation therapy. Tumour Biol. 2016;37:3469–77. [PubMed: 26449830]

[64]. Lynn H, Sun X, Bime C, Casanova N, Oita RC, Ramos N, et al. NAMPT haplotypes and plasma eNAMPT levels predict ARDS severity outcomes. American journal of physiology Lung cellular and molecular physiology. 2021 (submitted).

[65]. Beach TA, Groves AM, Williams JP, Finkelstein JN. Modeling radiation-induced lung injury: lessons learned from whole thorax irradiation. Int J Radiat Biol. 2020;96:129–44. [PubMed: 30359147]

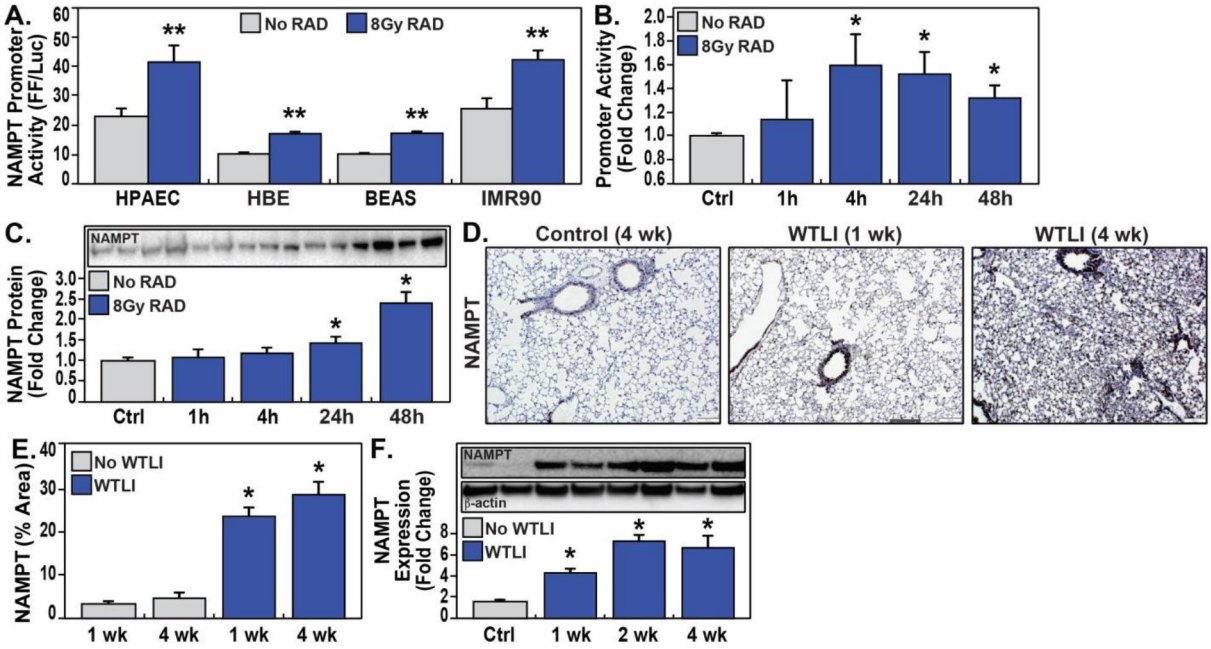

Figure 1. Radiation-induced NAMPT expression in human cells and murine lung tissues.

A. 8 Gy radiation exposure (24 hours) significantly increased *NAMPT* promoter luciferase reporter activities in lung endothelial cells (HPAEC), epithelial cells (HBE and BEAS), and fibroblasts (IMR90) (**p<0.01 each). **B.** 8 Gy-mediated increases in *NAMPT* promoter activities in lung epithelial cells (HBE) are time-dependent, peaking at 4 hours but remaining elevated at 48 hours (**p<0.01 each). **C.** Increased *NAMPT* promoter activities were accompanied by increased NAMPT protein content in human epithelial cells (HBE) exposed to 8 Gy radiation for 1, 4, 24 and 48 hrs. Cells were lysed with RIPA buffer and NAMPT protein detected by immunoblotting with rabbit anti-human NAMPT 1:10000 (BLR058F, Bethyl, Montgomery, TX), as we previously reported [25, 34]. Densitometry studies confirmed significantly increased NAMPT protein levels in HBEs after exposure to 8 Gy irradiation at 24 and 48 hours, compared non-irradiated controls. **D.** Immunohistochemical lung tissue staining with Image J quantification of NAMPT detected by immunoblotting with rabbit anti-human NAMPT (BLR058F, Bethyl, Montgomery, TX) as we previously reported [21] in C57BL/6J mice exposed to 20Gy WTLI. **E.** Western blotting of immunoreactive NAMPT in lung homogenates from control and 20 Gy WTLI-exposed murine lung tissues at 1, 2 and 4 weeks with densitometric measurements. Together, these results demonstrate significantly increased NAMPT expression at 1 week persisting at 2 and 4 weeks after WTLI compared to controls with expression intensity summarized by Image J software imaging or by densitometry.

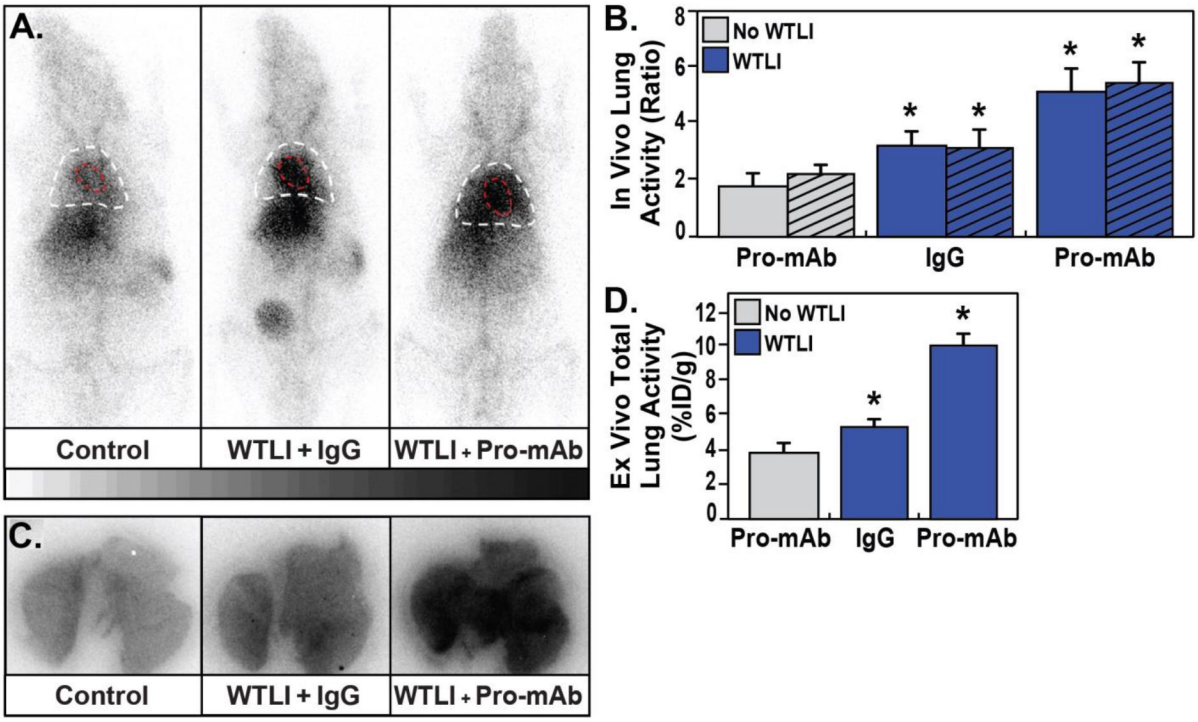

Figure 2. ***In vivo*** **imaging of NAMPT expression in preclinical radiation pneumonitis.**

A. Representative whole-body iQID images collected at 240 min post ^{99m}Tc-ProNamptor™ monoclonal antibody (Pro-mAb) and ^{99m}Tc-IgG (IgG) injection, respectively, in sham-IR, non-radiated mice (Ctrl) and 20 Gy-exposed (WTLI) C57BL/6J mice at 1 week. The entire chest region of interest (ROI) is outlined by the white dashed lines and the cardiac blood pool is outlined by the red dashed lines. The ROI volumes lying between the white and red dashed lines represents the lung volumes. These images represent specific increased WTLI-induced activity and NAMPT lung expression. **B.** A summary of the results of *in vivo* quantitative image analysis of radiolabeled Pro-mAb activity in control sham-IR mice (Ctrl, n=6) and in WTLI-exposed mice 1 week post WTLI exposure (n=7). Results were compared to ^{99m}Tc-IgG -exposed WTLI-exposed mice (n=5) 1 week post exposure. Results are expressed as a ratio of left or right lung ROI activity to the soft-tissue background activity (measured over the thigh region) (* $P < 0.05$ compared to Ctrl; Φ $P < 0.05$ compared to RILI 1-wk Pro-mAb for either left or right lungs). **C.** *Ex vivo* lung autoradiograph imaging confirmed the *in vivo* imaging findings, showing marked increased Pro-mAb uptake in the WTLI lungs, as compared to lungs of sham-IR (Ctrl Pro-mAb) or mice receiving non-specific ^{99m}Tc-IgG 1 week post WTLI exposure radiation. **D.** *Ex vivo* quantitative total-lung radioactivity of Pro-mAb and IgG measured and expressed as a percent of total injected dose per gram of tissue (%ID/g) at 1 week post WTLI exposure showing statistical differences in Pro-mAb lung uptake between the WTLI and control lungs. A 2.6-fold increase of Pro-mAb activity was observed in the mice at 1 week after radiation compared to Pro-mAb in Ctrl non-irradiated mice, and 1.9-fold higher than non-specific IgG lung activity at the same time after WTLI (P <0.05). The difference between non-specific IgG uptake in the 1 week post-irradiation mice and Pro-mAb in non-irradiated controls is statistically nonsignificant.* $P < 0.05$ compared to Ctrl; Φ $P < 0.05$ compared to RILI 1-wk Pro-mAb.

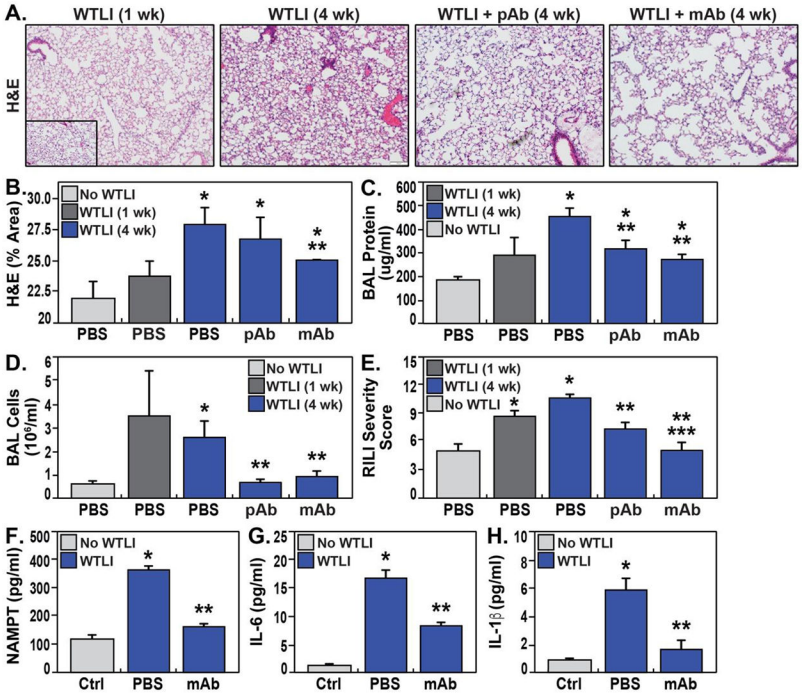

Figure 3. eNAMPT neutralization reduces the severity of preclinical radiation pneumonitis.

A/B. Compared to sham-IR exposed C57BL/6J mice (inset), H&E staining revealed marked increases in vascular leakage, leukocyte infiltration and inflammatory lung injury in WT mice exposed to 20Gy radiation at 1 and 4 weeks post WTLI exposure (quantified by quantified by Image J analysis). WTLI 20Gy-exposed WT mice receiving either the eNAMPT-neutralizing pAb (4mg/kg, weekly intraperitoneally) or humanized mAb (0.4mg/kg, weekly intraperitoneally) demonstrated significant histologic reductions in WTLI-mediated inflammatory lung injury with the humanized eNAMPT mAb significantly more protective than the eNAMPT pAb compared to the PBS/IgG_1 control. **C/D.** Both WTLI-mediated BAL protein levels and BAL cells were increased at 1 week post WTLI with further significant increases observed at 4 weeks. Consistent with the histologic protection noted in panel A/B, eNAMPT-neutralizing pAb and mAb treatments produced marked reductions in WTLI-mediated BAL protein levels and BAL cells assessed 4 weeks post WTLI exposure. **E.** Evaluation of the Radiation-Induced Lung Injury Severity Score (RILISS), integrating inflammatory indices (H&E staining, BAL protein and cells), demonstrates an overall 60% reduction in RILISS by eNAMPT-neutralizing pAb and mAb treatments. The humanized mAb again provided significantly greater protection against WTLI-induced pneumonitis than the eNAMPT pAb. **F/G/H.** The MesoScale ELISA-based Discovery platform was utilized to assess eNAMPT neutralization effects on plasma cytokine levels in preclinical radiation pneumonitis. Depicted are mouse plasma levels of eNAMPT (**F**), and the inflammatory cytokines IL-6 (**G**) and IL-1b (**H**) obtained in control sham-IR exposed mice (n=5), untreated 20 Gy WTLI-exposed mice receiving weekly IP PBS/IgG_1 (n=7, 4 weeks) and WTLI-exposed mice receiving the eNAMPT-neutralizing mAb weekly IP (n=7, 4 weeks). Exposure to 20 Gy WTLI marked increases plasma eNAMPT, IL-6 and IL-1b levels which are significantly reduced by the eNAMPT-neutralizing mAb.

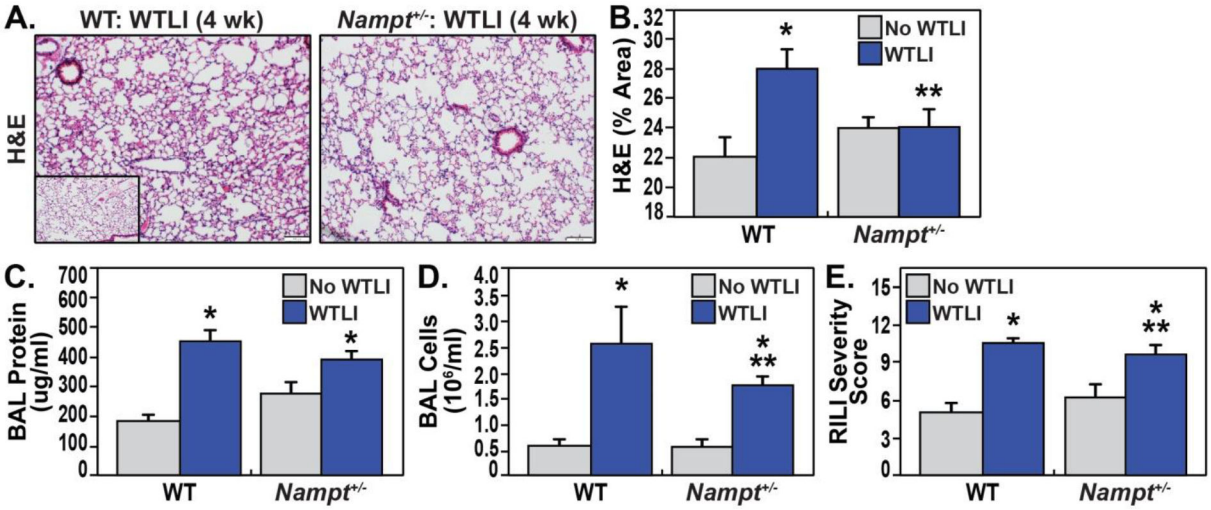

Figure 4. *Nampt*$^{+/-}$ heterozygous mice are protected from preclinical radiation pneumonitis.

A/B. Shown is histologic evidence (H&E staining) of moderately severe inflammatory lung injury in WTLI (20Gy)-exposed C57BL/6J wild type mice at 4 weeks compared to sham-IR exposed mice **(inset).** In contrast, WTLI-exposed *Nampt*$^{+/-}$ heterozygous mice exhibited significantly reduced histologic inflammation and injury compared to WT mice, with quantification by Image J software. **C/D.** WTLI-exposed *Nampt*$^{+/-}$ heterozygous mice (4 weeks) demonstrated significant increases in total BAL protein levels and BAL cells (* $p< 0.05$). When compared to WTLI-exposed WT mice, the total number of BAL cells was significantly reduced (** $p<0.01$) as was total BAL protein without reaching statistical significance. **E.** Comparison of WTLI-induced lung injury scores (RILISS) (4 weeks) revealed significantly increased RILISS in both WT and *Nampt*$^{+/-}$ heterozygous mice compared with sham-IR exposed mice (* $p<0.01$) but with RILISS significantly reduced in *Nampt*$^{+/-}$ heterozygous mice compared to WT mice (** $p<0.01$).

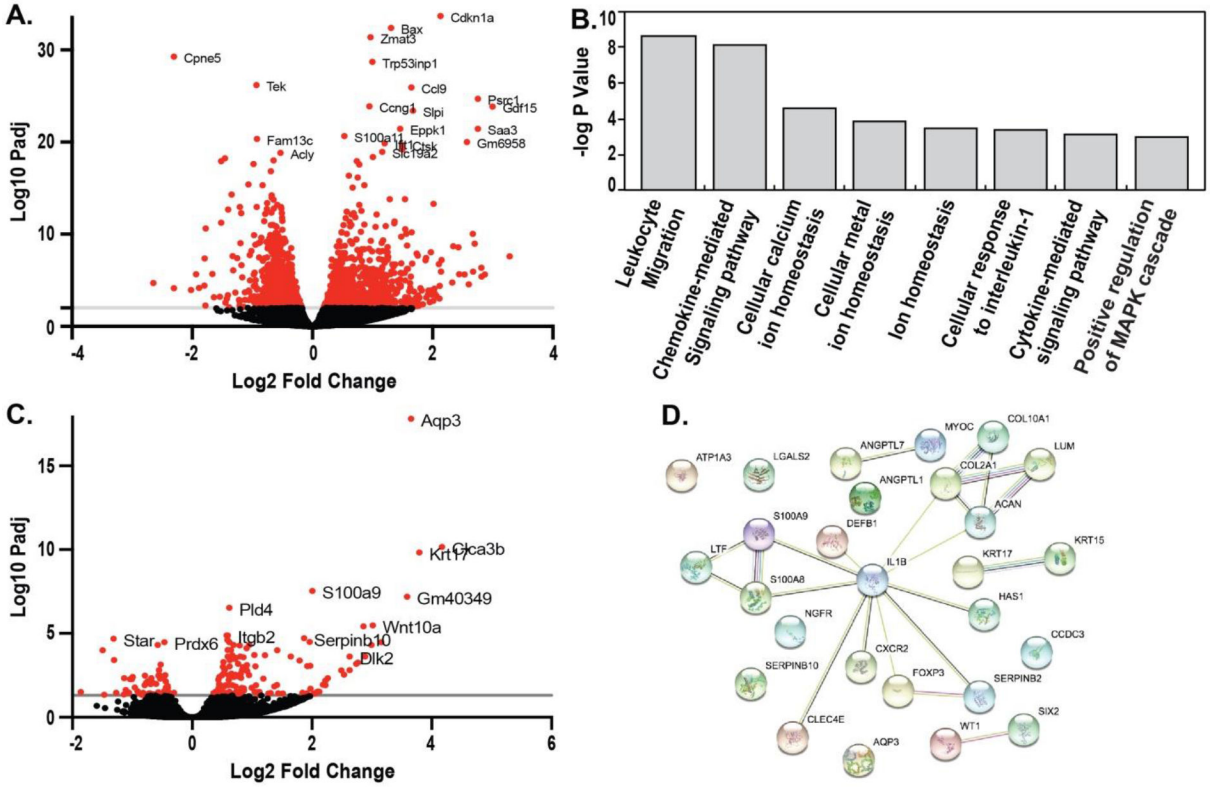

Figure 5. Genomic interrogation of dysregulated genes/signaling pathways in preclinical radiation pneumonitis: effect of eNAMPT neutralization.

A. RNA sequencing of WTLI-exposed lung tissues (4 week) was performed and compared to non-radiated control mice. Shown is a volcano plot depicting the differentially-expressed genes (DEGs) with the X axis representing log2 transformed fold change (FC). A total of 2325 DEGs exhibiting a FDR < 0.01 and 336 exhibited a FC >1.0 (289 genes) or l <1.0 (47 genes). The top 4 upregulated genes with FC >1.5: *MMP12* (−log10padj =82.2), *Phida3* (−log10padj =60.8, *Aen* (−log10padj =46), and *Eda2r* (−log10padj =43.6) are not depicted. **B.** Shown are the top GO biologic processes (molecular function) identified by STRING analysis of the 336 DEGs. Highlighted are the MAP kinase signaling and cytokine- and chemokine-mediated signaling. **C.** The role of circulating eNAMPT in driving dysregulated lung inflammatory signaling and injury/repair processes was assessed by RNA sequencing of lung tissues from WTLI-exposed mouse lung tissues (4 week) with and without eNAMPT mAb treatment. Shown is a volcano plot depicting the 207 DEGs filtered from exhibiting a FDR < 0.05 (far fewer DEGs than in Panel A), with 55 genes exhibiting FCs >1.0 and 12 with FCs <1.0). **D.** STRING interaction networks of the 67 significant eNAMPT-influenced DEGs (adjusted p<0.05, FC +/− 1). Network nodes represent proteins and the edges indicate the functional association, the line thickness indicates the strength of the data support. These analyses highlighted a very strong signal for IL-1b as a hub of eNAMPT mAb-influenced interacting genes.

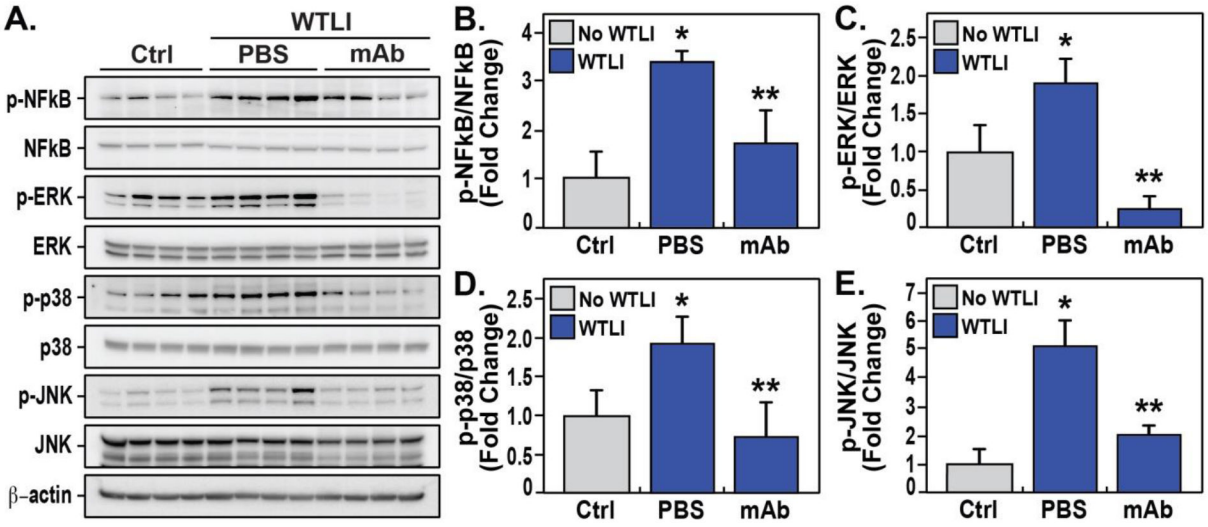

Figure 6. eNAMPT neutralization attenuates dysregulated signaling pathways in preclinical radiation pneumonitis.

A. Compared to sham-IR-exposed mice (n=3), Western blot studies of lung tissue homogenates from WTLI-exposed, PBS/IgG-treated mice (n=5, 4 weeks) showed prominent phosphorylation of NFKB compared to total NFkB protein content (total β-actin as loading control). In contrast, phospho-NFKB protein content was markedly reduced in WTLI-exposed mice (n=5) receiving the eNAMPT-neutralizing mAb (0.4mg/kg, weekly) compared with PBS/IgG-treated mice. These results were captured by densitometric evaluation of the ratio of p-NFkB/NFkB (fold change) (*p<0.05 control vs. untreated WTLI; **p<0.05 mAb WTLI vs. untreated WTLI). **B.** Similar to Panel 7A, lung tissue homogenates from control and WTLI-exposed mice (n=5, 4 weeks) were evaluated for MAP kinase family activation by levels of ERK, JNK p38 phosphorylation. These studies demonstrated robust MAP kinase family pathway activation as evidenced by protein phosphorylation (pp-p38, pp-JNK, pp-42/44 ERK) which was reversed by treatment with the eNAMPT-neutralizing mAb, results captured by densitometric evaluation. *p<0.05 control vs. untreated WTLI; **p<0.05 mAb WTLI vs. untreated WTLI.

Table 1.

Differentially-expressed genes in KEGG/Reactome pathways:
Control vs WTLI-exposed mice (4 weeks).

Pathway	Set Size	Candidates	p-value	q-value	Pathway Source
Oxidative phosphorylation	134	57 (42.5%)	3.87E-11	2.53E-08	KEGG
Pathways in cancer	530	148 (27.9%)	9.54E-09	2.23E-06	KEGG
Transcriptional misregulation in cancer	183	63 (34.6%)	6.80E-08	1.24E-05	KEGG
Respiratory electron transport, ATP synthesis/heat production	86	37 (43.0%)	7.11E-08	1.24E-05	Reactome
P53 signaling pathway	71	31 (43.7%)	3.42E-07	7.61E-05	KEGG
Rap1 signaling pathway	209	37 (32.1%)	6.97E-07	8.88E-05	KEGG
Signaling by Receptor Tyrosine Kinases	377	104 (27.7%)	2.20E-06	2.37E-04	Reactome
Hepatocellular carcinoma	171	56 (32.7%)	2.68E-06	2.68E-06	KEGG
Chemokine signaling pathway	199	60 (31.2%)	4.47E-06	5.70E-04	KEGG
Phospholipase D signaling	147	48 (32.9%)	1.20E-05	9.41E-04	KEGG
Rho GTPase cycle	138	46 (33.3%)	1.21E-05	9.41E-04	Reactome
Neutrophil degranulation	565	139 (25.0%)	1.95E-05	1.37E-03	Reactome
Fc gamma R-mediated phagocytosis –	87	32 (37.2%)	2.16E-05	1.44E-03	KEGG

Table 2.

Top STRING GO-related terms associated to molecular function:
WTLI mice- PBS/IgG vs eNAMPT-neutralizing mAb (4 weeks).

Term	Gene Count	Background Genes	FDR	Matching Members
Toll-like receptor 4 binding	2	3	0.016	S100a8,S100a9
MHC class II protein binding	2	6	0.0167	Krt17,Col2a1
Signaling receptor binding	11	1513	0.026	Myoc,Angptl1,Wnt10a,Il1b,Defb1,Krt17,S 100a8,S100a9,Col2A1,Agr2,Adh7
ECM structural constituent	3	73	0.026	Emilin2,Lum,Acan
Lipid binding	7	673	0.0311	Ltf, Star, S100a8, S100a9,Dmbt1,Adh7,Atp1A3

Table 3.

Differentially-expressed genes in KEGG/Reactome Pathways:
WTLI mice- PBS/IgG vs eNAMPT mAb (4wks).

Pathway Name	Set Size	Candidates	p-Value	q Value	Pathway Source
Innate Immune System	9.94E+02	45 (4.6%)	1.89E-17	2.55E-15	Reactome
Neutrophil degranulation	5.65E+02	32 (5.8%)	4.19E-15	2.83E-13	Reactome
Immune System	1.66E+03	49 (3.0%)	1.04E-11	4.67E-10	Reactome
RHO GTPases Activate NADPH Oxidases	1.30E-01	4 (30.8%)	8.93E-06	0.000201	Reactome
Hemostasis	5.85E+02	19 (3.2%)	1.88E-05	0.000362	Reactome
Leukocyte transendothelial migration	1.15E+02	8 (7.0%)	3.37E-05	0.000569	KEGG
GPVI-mediated activation cascade	3.20E+01	4 (12.5%)	0.000382	0.0042	Reactome
Detoxification of Reactive Oxygen Species	3.50E+01	4 (11.4%)	0.000543	0.00564	Reactome
Fc gamma R-mediated phagocytosis	9.80E+01	6 (6.1%)	0.000694	0.00669	Reactome
Antigen processing-Cross presentation	4.20+01	4 (10.3%)	0.000825	0.00742	Reactome
Antimicrobial peptides	7.40E+01	5 (7.2%)	0.000916	0.00773	Reactome
DAP12 signaling / interactions	4.10E+01	4 (9.8%)	0.000998	0.00783	Reactome
VEGFA-VEGFR2 Signaling Pathway	8.30E+01	5 (6.0%)	0.0021	0.0123	Reactome
Semaphorin interactions	5.10E+01	4 (7.8%)	0.00227	0.0127	Reactome
Adaptive Immune System	6.18E+02	15 (2.4%)	0.00284	0.0148	Reactome
Chemokine signaling pathway	1.99E+02	7 (3.6%)	0.00503	0.0226	KEGG